

**Low-temperature thermal conductivity of cryocrystals formed by linear three-atom molecules**V. V. Sumarokov,<sup>1,2</sup> P. Stachowiak,<sup>1</sup> J. Mucha,<sup>1</sup> and A. Jeżowski<sup>1</sup><sup>1</sup>*Institute of Low Temperature and Structure Research, Polish Academy of Sciences, P.O. Box 1410, 50-950 Wrocław, Poland*<sup>2</sup>*B. Verkin Institute for Low Temperatures and Engineering, National Academy of Sciences of Ukraine, 47 Lenin Avenue, Khar'kov, Ukraine*

(Received 19 April 2006; revised manuscript received 2 October 2006; published 20 December 2006)

Thermal conductivity of CO<sub>2</sub> and N<sub>2</sub>O solids has been investigated over the temperature range 1–40 K. The thermal conductivity coefficient of CO<sub>2</sub> and N<sub>2</sub>O exhibits, in the whole investigated temperature range, surprisingly high value when compared with other N<sub>2</sub>-type molecular crystals. Analysis of the experimental data, in framework of the Debye model, indicates that relatively big size of the crystal grains, low density of dislocations and weak phonon–phonon interaction might be reasons for the good thermal conduction in these crystals at temperatures near the maximum of the thermal conductivity. It has been found that there is an additional (in comparison with CO<sub>2</sub>) significant mechanism of scattering of phonons in N<sub>2</sub>O. Supposedly this scattering occurs on the end-to-end disordered N<sub>2</sub>O molecules.

DOI: [10.1103/PhysRevB.74.224302](https://doi.org/10.1103/PhysRevB.74.224302)

PACS number(s): 63.20.-e, 66.70.+f

**I. INTRODUCTION**

Solid carbon dioxide (CO<sub>2</sub>) and nitrous oxide (N<sub>2</sub>O) belong to the group of N<sub>2</sub>-type simple molecular crystals (N<sub>2</sub>, CO, CO<sub>2</sub>, and N<sub>2</sub>O). CO<sub>2</sub> and N<sub>2</sub>O crystals are built out of linear three-atom molecules (O–C–O and N–N–O). These crystals, like the rare-gas solids and diatomic solids, are the simplest materials with regard to structure, lattice dynamics, and other physical properties. Relative simplicity of nitrous oxide and carbon dioxide crystals and their model character have stimulated intense investigation, both theoretical and experimental, of their physical properties (see, e.g., Refs. 1–10). Among these two solids, several of their basic crystal parameters such as molecular mass, heat of sublimation, zero-point energy, Debye temperature, nearest-neighbor distance, and rotational constant exhibit very similar values.

At the equilibrium vapor pressure, CO<sub>2</sub> and N<sub>2</sub>O crystals have *Pa3* structure (below their triple point temperatures 216.57 K and 182.35 K,<sup>7,8</sup> respectively). The axes of molecules in these crystals are oriented along the body diagonals of the cubic elementary cell. The basic difference between CO<sub>2</sub> and N<sub>2</sub>O is that the molecule of N<sub>2</sub>O, contrary to the CO<sub>2</sub> molecule, is not symmetric with respect to ends reversal and thus possesses a nonzero dipolar moment. At higher temperatures, molecules of crystalline N<sub>2</sub>O are disordered with respect to the O-end position.<sup>11</sup> The problem of dipole ordering in nitrous oxide crystal has been widely discussed (see, e.g., Refs. 7 and 9–12). There is a theoretical estimation<sup>10</sup> of the temperature (11 K) of the possible structural phase transition into the phase with dipole ordering. Atake and Chihara<sup>3</sup> precisely determined (from their own calorimetric studies) the value of the residual entropy (difference between spectroscopic and calorimetric entropies)  $\Delta S_{res}/R \ln 2 = 1.04 \pm 0.17$  (see also Ref. 7, and references therein), which suggests that the N<sub>2</sub>O crystal is in nonequilibrium state which is kinetically frozen at low temperatures. It is supposed that the residual entropy appears in N<sub>2</sub>O solid because of the frozen dipole disorder. The value of the residual entropy obtained by the cited authors evidences that N<sub>2</sub>O crystal is totally end-to-end disordered.

The thermal conductivity data for crystalline CO<sub>2</sub> and N<sub>2</sub>O at equilibrium vapor pressure have already been published for temperatures above ~25 K.<sup>4</sup> Earlier, we have also reported our preliminary experimental results of thermal conductivity of CO<sub>2</sub> and N<sub>2</sub>O solids in the temperature range 1–40 K.<sup>13,14</sup> It has been found that the value of the coefficient of thermal conductivity of CO<sub>2</sub> in maximum<sup>14</sup> is considerably higher than the maximum value of thermal conductivity of N<sub>2</sub>O.<sup>13</sup> The conditions of the preparation of CO<sub>2</sub> and N<sub>2</sub>O samples in these works<sup>13,14</sup> were different. Therefore, it is interesting to investigate the thermal conductivity of the crystalline sample of N<sub>2</sub>O prepared in the same way as CO<sub>2</sub> solid.

The purpose of the current paper is to present experimental data of the thermal conductivity of N<sub>2</sub>O solid, to compare them with previously obtained data of thermal conductivities of CO<sub>2</sub> and N<sub>2</sub>O solids,<sup>13,14</sup> and to discuss all the results in more detail.

**II. EXPERIMENT**

For clarity of presentation, the conditions of the crystals preparation are briefly described, both for the presented here experiment and our previous papers.<sup>13,14</sup>

The crystalline samples CO<sub>2</sub> and N<sub>2</sub>O were obtained by the method of condensation of gas on a cold substrate.

The samples of studied cryocrystals have been grown and measured in a cylindrical glass ampoule. The inner diameter was equal to 4.2 mm, the wall thickness—1.0 mm, and the length—36 mm.

The sample of CO<sub>2</sub> reported in Ref. 14 was grown under the following conditions of condensation: the temperature—~173.3 K, the pressure—~14 kPa, the crystal growth rate ~1.5 mm/h. Temperature gradient of ~2.2 K/cm along the ampoule was maintained during the condensation. When the crystal filled the ampoule completely, the process was terminated and the temperature gradient slowly reduced to about 1.1 K/cm. Next, the sample was cooled at the rate of about 0.1 K/h in the temperature range 173–100 K, ~0.2 K/h in the range 100–70 K and ~0.5 K/h below 70 K.

The conditions of the growth of the crystalline samples of  $N_2O$  reported in Ref. 13 were as follows: the condensation temperature—162 K, the temperature gradient along the ampoule—1.7 K/cm, and the crystal growth rate—around 1.5 mm/h. Once the solid  $N_2O$  filled the ampoule, the crystal was annealed for 12 h at the temperature of the growth. Then the sample was cooled to the temperature of liquid helium at the rate of 1 K/h. The obtained in the reported here experiment sample of the  $N_2O$  crystal has been grown under the same conditions as the previous (Ref. 13)  $N_2O$  samples. However, the cooling conditions were changed and were similar to those for  $CO_2$  solid.<sup>14</sup>

The technique of this experiment makes impossible any structural investigation of the samples of solidified gas prepared for the thermal conductivity measurements. The samples have been merely inspected visually through special windows in the measurement chamber of the setup. During the sample growth one could observe the gas-crystal interface and the crystal gradually, tightly filling in the ampoule, beginning from its bottom, without any voids. The samples of  $CO_2$  and  $N_2O$  crystals have been transparent without visible defects after cooling down to helium temperatures.

To improve the thermal contact of the crystal with thermometers and the gradient heater, the heat-exchanging gaseous  $^4He$  was admitted to the ampoule at the pressure of 1 kPa.

Both  $CO_2$  and  $N_2O$  gases used in the experiment had natural isotopic composition and contained impurities of concentration not exceeding 0.001%. The purity has been checked by means of a mass spectrometer before the experiment. When the measurements have been completed, each sample was evaporated and the amount of impurities was checked again by the same means.

The measurements of the thermal conductivities of  $N_2O$  and  $CO_2$  crystals have been made by the steady state flow method in the temperature range 1.2–40 K and 1.5–36 K, respectively.

For the measurement of temperature of the samples and the temperature gradient along them, two calibrated germanium thermometers have been used. The thermometers were attached to the ampoule with aid of thin copper rings. The rings were fixed with a heat conducting glue in semicircular channels carved in the ampoule walls in the planes perpendicular to the ampoule axis. The distance between the thermometers along the ampoule was 12 mm, the lower thermometer being positioned about 9 mm from the bottom of the ampoule. To take into account the amount of heat transferred by the ampoule wall, the thermal conductivity coefficient dependence on the temperature of the glass was determined in a separate experiment.

The statistical error of the measurement of the thermal conductivity did not exceed 7% in the whole temperature range. The main source of the error at low temperatures was the uncertainty of specifying small measured temperature gradients, whereas at high temperatures—the long-term instability of temperature-controlling devices. The systematic error, originating mainly from inaccuracy of determination of the sample dimensions, did not exceed 3%.

Other details of the experiment were described in Refs. 15–17.

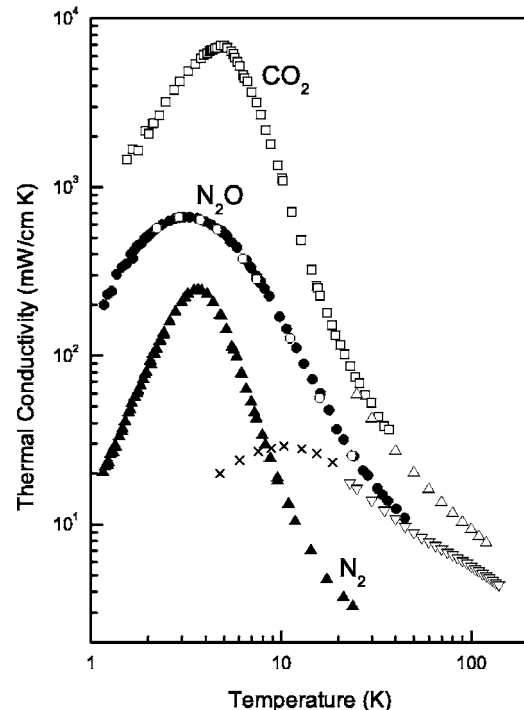


FIG. 1. Temperature dependence of thermal conductivity of the solid  $CO_2$ ,  $N_2O$ , and  $N_2$  samples. Our experimental data:  $\circ$ — $N_2O$ , the present work,  $\bullet$ — $N_2O$  from Ref. 13,  $\times$ — $N_2O$  (an imperfect sample) from Ref. 13,  $\square$ — $CO_2$  from Ref. 14,  $\blacktriangle$ — $N_2$  from Ref. 16, and literature data:  $\triangle$ — $CO_2$  and  $\nabla$ — $N_2O$  from Ref. 4.

### III. RESULTS AND DISCUSSION

The data of thermal conductivity for the sample of crystalline  $N_2O$  obtained in the reported experiment have been depicted in Fig. 1. Additionally, our previous experimental results of the temperature dependence of the thermal conductivity coefficient  $\kappa$  for  $N_2O$  (Ref. 13) and  $CO_2$  (Ref. 14) solids are shown in Fig. 1. For comparison, earlier literature data of  $\kappa(T)$  for carbon dioxide and nitrous oxide crystals by Koloskova *et al.*<sup>4</sup> and  $\kappa(T)$  for crystalline nitrogen<sup>16</sup> have also been depicted in Fig. 1. As can be seen from Fig. 1, the results of measurement of thermal conductivity of the  $N_2O$  crystal obtained in this work do not practically diverge from the ones of the previous samples.<sup>13</sup> Thus we conclude that the great difference between low-temperature thermal conductivity of  $N_2O$  and  $CO_2$  crystals does not result from their preparation procedure.

The obtained experimental temperature dependence of  $\kappa$  for  $CO_2$  and  $N_2O$  solids are typical for a dielectric crystal. Attention is drawn to the fact that the thermal conductivity coefficient of these cryocrystals reaches very high value. The maximum value of the thermal conductivity coefficient  $\kappa$  is  $7200 \text{ mW cm}^{-1} \text{ K}^{-1}$  for solid  $CO_2$  and  $\approx 700 \text{ mW cm}^{-1} \text{ K}^{-1}$  for solid  $N_2O$ , at temperatures 5 and 3.1 K, respectively. The values of thermal conductivities of  $CO_2$  and  $N_2O$  crystals are much greater than those for any other simple molecular crystal (see Refs. 16–18). For example, the thermal conductivity of nitrous oxide crystal at the maximum is several times higher, and the one of the  $CO_2$  crystal is several tens times higher than that of solid  $N_2$  (see Fig. 1). The discrepancy

TABLE I. The relaxation rates for the different mechanisms of phonon scattering (Ref. 20) [scattering on grain boundaries, on dislocation stress fields, on point defects, and on phonons (the Umklapp three-phonon processes)].

Scattering mechanism	Relaxation rate
Grain boundaries	$\tau_b^{-1} = a_b$
Dislocations (strain fields)	$\tau_d^{-1} = a_d x T$
Isotopic impurities	$\tau_p^{-1} = a_p x^4 T^4$
U-process	$\tau_u^{-1} = a_{1u} x^2 T^5 \exp[-a_{2u}/T]$

between thermal conductivity of crystalline  $N_2$  and presented in this article data for  $CO_2$  and  $N_2O$  crystals will be discussed in Sec. III C of the current section.

The values of the thermal conductivity coefficient of  $CO_2$  and  $N_2O$  of Ref. 4 are lower than our results, the difference increasing with decreasing temperature. We suppose that it is varying the degree of imperfection of the samples which is responsible for the difference. The results of measurements of  $\kappa$  of our imperfect (due to a thermal shock during cooling) sample of  $N_2O$  crystal, depicted in Fig. 1, evidences in favor of this supposition. As seen from Fig. 1, the experimental results of thermal conductivity of this imperfect sample merge with Koloskova *et al.*'s data.<sup>4</sup> Note also that in the past Kimber and Rogers<sup>19</sup> observed a similar depression of the thermal conductivity for solid neon caused by a thermal shock.

The results of our measurements were analyzed using the relaxation time method in the framework of the Debye model. The expression for thermal conductivity of a dielectric crystal can be written as (Ref. 20)

$$\kappa = GT^3 \int_0^{\theta/T} \tau_r x^4 e^x (e^x - 1)^{-2} dx. \quad (1)$$

In this expression

$$G = \frac{k_B^4}{2\pi^2 v \hbar^3}, \quad x = \frac{\hbar \omega}{k_B T},$$

$k_B$ —the Boltzmann constant,  $\hbar = h/2\pi$ ,  $h$ —the Planck constant,  $\omega$ —phonon frequency,  $\theta \equiv \Theta_D$ —the Debye characteristic temperature,  $\tau_r$ —the relaxation time for resistive phonon interactions,  $v = [\frac{1}{3}(v_l^{-3} + 2v_t^{-3})]^{-1/3}$ —the sound velocity averaged over longitudinal  $v_l$  and transversal  $v_t$  polarizations.<sup>21</sup>

With the assumption that scattering processes of different types do not influence each other, the relaxation time  $\tau_r$  may be written down as follows:

$$\frac{1}{\tau_r} = \frac{1}{\tau_b} + \frac{1}{\tau_p} + \frac{1}{\tau_d} + \frac{1}{\tau_u}. \quad (2)$$

The relations of relaxation rates as a function of phonon frequency for various scattering mechanisms used in the present analysis are given in Table I.

In the course of analysis of the low-temperature part of the experimental results, only the scattering processes mentioned in Table I were taken into consideration. Since the

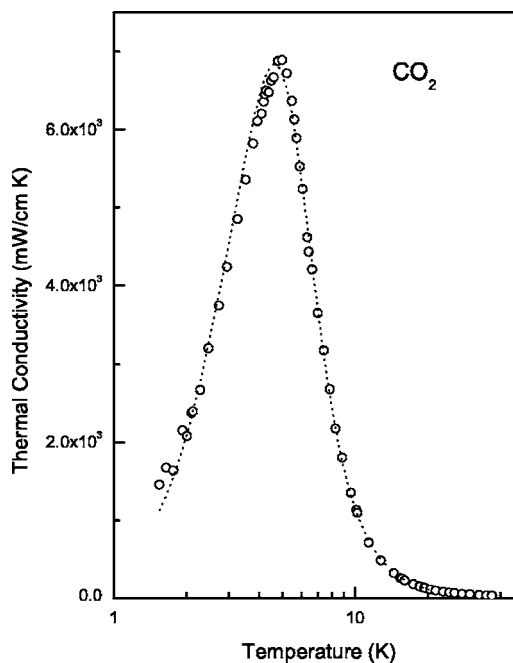


FIG. 2. Low-temperature thermal conductivity of the  $CO_2$  crystals.  $\circ$ —our experimental data from Ref. 14. Dotted line is the result of fitting.

lowest energy level of excitation of the librations corresponded to  $74.8 \text{ cm}^{-1}$  ( $\sim 105 \text{ K}$ ) and  $69.3 \text{ cm}^{-1}$  ( $\sim 100 \text{ K}$ ) for  $CO_2$  and for  $N_2O$ , respectively (cf., e.g., Ref. 7), neither the contribution of librations into heat transport nor the scattering of phonons on librations were taken into account.

The fitting procedure described in Ref. 16 was used, i.e., the parameters  $a_j$  ( $j = b, p, d, 1u, 2u$ ), appearing in Table I, were found by minimizing the functional  $\sum_i [(\kappa_{\text{calc } i} - \kappa_{\text{exp } i}) / \kappa_{\text{exp } i}]^2$  where  $\kappa_{\text{calc } i}$  and  $\kappa_{\text{exp } i}$  were, respectively, the calculated (1) and experimental values of the thermal conductivity coefficient at  $i$ th temperature point.

For calculations, the values from Ref. 7:  $\Theta_D = 141 \text{ K}$ ,  $v_l = 2676.3 \text{ m/s}$ ,  $v_t = 1513.1 \text{ m/s}$ , and  $\Theta_D = 151.8 \text{ K}$ ,  $v_l = 2806.4 \text{ m/s}$ ,  $v_t = 1605.7 \text{ m/s}$ , for  $N_2O$  and  $CO_2$ , respectively, were used.

### A. Carbon dioxide

The experimental temperature dependence of the thermal conductivity of solid  $CO_2$  is described by Eq. (1) with expression (2) for  $\tau_r$  in the temperature range below  $\sim 20 \text{ K}$ . As a result of the fitting procedure, the following parameters  $a_j$  have been obtained:

$$\begin{aligned} a_b &= 1.110 \times 10^5 \text{ s}^{-1}, & a_d &= 7.414 \times 10^4 \text{ s}^{-1} \text{ K}^{-1}, \\ a_p &= 24.85 \text{ s}^{-1} \text{ K}^{-4}, & a_{1u} &= 1.575 \times 10^3 \text{ s}^{-1} \text{ K}^{-5}, \\ a_{2u} &= 19.56 \text{ K}. \end{aligned} \quad (3)$$

The obtained approximate temperature dependence of the thermal conductivity of solid  $CO_2$  has been shown in Fig. 2. As may be seen in Fig. 2, this curve satisfactorily describes

the experimental data. The contributions of different mechanisms into the phonon scattering have been estimated. Figure 3 displays the ratio ( $\tau_i^{-1}/\tau_r^{-1} = \tau_r/\tau_i$ ) of the relaxation rate for the individual scattering process  $\tau_i^{-1}$  ( $i=b,d,p,u$ ) to the resistive relaxation rate  $\tau_r^{-1}$  versus the phonon energy for different temperatures from 2 K up to 10 K for the CO<sub>2</sub> crystal. The indexes  $b$ ,  $d$ ,  $p$ , and  $u$  correspond to the scattering of phonons on grain boundaries, on dislocation stress fields, on point defects, and on phonons (the U-processes), respectively. As seen from Fig. 3, the relaxation rate of the scattering of phonons on dislocation and boundary scattering contributes significantly to the relaxation rate of resistive processes for phonons with energy  $E_{\text{ph}} < 10\text{--}20$  K at  $T < 7$  K. The contribution of the point defects scattering prevail for phonons with  $E_{\text{ph}} > 10$  K at  $T < 10$  K. The contribution from U-processes begin to dominate over others at  $T > \sim 6\text{--}7$  K.

Using the expressions from Table I, the average size of the crystallites, the densities of dislocations, and point defects were estimated. From expression

$$\tau_b = \frac{L}{v} \quad (4)$$

the value of the average size  $L$  of a crystallite has been obtained. The average dimension of crystallites  $L$  thus estimated is equal to about 16.1 nm and, hence, greater than the value of sample diameter.

Casimir obtained formula (4) for the relaxation rate of boundary scattering of phonons for a case when walls of a long crystalline sample scattered phonons in a diffuse manner.<sup>22</sup> However, phonon scattering may occur on smooth boundaries. Here, one can estimate a fraction of diffusive collisions of phonons with boundaries. The relation between the value of the thermal conductivity in a case of smooth boundary scattering and the one in a case of diffusion boundary scattering is presented in the literature (see, e.g., Ref. 20). This relation is equal to  $(2-F)/F$ , where  $F$  is the part of diffusive collisions with sample boundaries. Let us assume that for our crystal, in a case of diffuse scattering on boundaries, the mean free path is equal to the diameter of the sample. This way, one finds that the diffusive fraction of collisions of phonons with sample boundaries is equal to about 30%.

Despite high maximum value of the thermal conductivity, the dependence  $\kappa(T)$  for CO<sub>2</sub> sample for temperatures below maximum is far from temperature dependence of thermal conductivity for a perfect dielectric crystal. In the case of a dielectric crystal with low density of point defects and dislocations, the low-temperature thermal conductivity is specified by dominating scattering of phonons on grain or sample boundaries, which give  $k \sim T^3$ . In the case of our CO<sub>2</sub> sample this dependence is  $\kappa \sim T^{1.7}$ . Such dependence is close to that observed in the case of prevailing scattering of phonons on dislocation strain fields.<sup>9</sup> Indeed, as may be seen in Fig. 3, at low temperatures and for low-energy phonons, the dislocation scattering provides the main contribution to the relaxation rate of resistive processes.

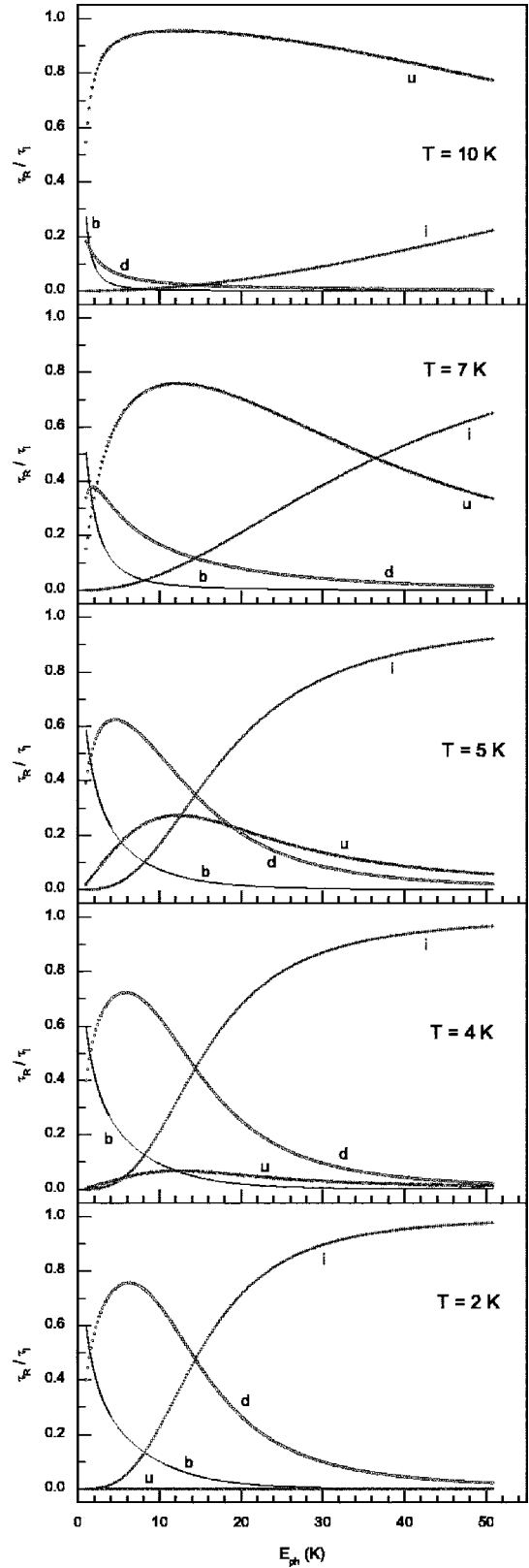


FIG. 3. Ratio of the relaxation rate for the individual scattering processes  $\tau_i^{-1}$  ( $i=b,d,i,u$ ) to the resistive relaxation rate  $\tau_r^{-1}$  for different temperatures for CO<sub>2</sub> crystal versus the phonon energy. Scattering of phonons:  $b$ —on grain boundaries,  $d$ —on dislocation stress fields,  $i$ —on point defects,  $u$ —on phonons (the U-processes).

The density of dislocations have been estimated from the equation

$$\tau_d^{-1} \propto \frac{N_d \gamma^2 \vec{B}^2 \omega}{2\pi} \quad (5)$$

for phonon scattering on strain fields of dislocations<sup>20</sup> ( $N_d$  is the dislocation density,  $\gamma$  is the Grüneisen constant,  $\vec{B}$  is the Burgers vector of the dislocation). From comparison of the expressions of  $\tau_d^{-1}$  from Table I and (5), using the value of  $a_d$  from (3),  $\gamma=2.13$  (Ref. 7) and  $B \sim a$  ( $a=5.5542 \text{ \AA}$ ),<sup>7</sup> the value of the dislocation density  $N_d=2.5 \times 10^8 \text{ cm}^{-2}$  was obtained.

To determine the point-defect density  $N_p$  expression (Ref. 20)

$$a_p = N_p k_B^4 v_a \frac{(\overline{\Delta M}/M)^2}{4\pi \hbar^4 v^3} \quad (6)$$

has been used, where  $v_a$  is the volume occupied by a molecule in the lattice,  $M$  is the molecule mass, and  $\overline{\Delta M}$  is the average mass defect. The obtained value of point-defect density  $N_p \approx 8.2\%$  is larger than the amount of isotope impurities. The overestimate of the value of  $N_p$  can be caused by ignoring in the expression for  $a_p$  the vacancy contribution in the mass defect and the contributions associated with the local variations of field constants and local distortions of the lattice.

### B. Nitrous oxide

First, in analyzing the data shown in Fig. 1 it is important to notice that in terms of quality the dependence  $\kappa(T)$  obtained for  $\text{N}_2\text{O}$  crystal differs from those for  $\text{CO}_2$  and  $\text{N}_2$ . The maximum, unlike in case of carbon dioxide and nitrogen crystals, is broad and circular, and the thermal conductivity for temperatures below the maximum does not show a power temperature dependence [the low-temperature part of the  $\kappa(T)$  for  $\text{N}_2$  and  $\text{CO}_2$  in the log-log coordinates can be approximated by straight lines while for  $\text{N}_2\text{O}$  cannot].

We tried to describe the experimental results of the thermal conductivity of  $\text{N}_2\text{O}$  crystal by means of expressions (1) and (2) only. The obtained fitting curve is shown in Fig. 4 (curve 1). As seen in Fig. 4, the experimental results are not described satisfactorily by curve 1. From the failure and the qualitative analysis of the  $\kappa(T)$  dependencies given above one can come to the conclusion that in the  $\text{N}_2\text{O}$  crystal there is an additional mechanism of significant scattering of phonons, absent from  $\text{CO}_2$  crystal.

It was supposed that such additional scattering of phonons occurs on the end-to-end disordered molecules  $\text{N}_2\text{O}$ . Hence, a term  $1/\tau_a$  shall be added to the right side of expression (2) describing this additional scattering:

$$\frac{1}{\tau_r} = \frac{1}{\tau_b} + \frac{1}{\tau_p} + \frac{1}{\tau_d} + \frac{1}{\tau_u} + \frac{1}{\tau_a}. \quad (7)$$

The experimentally obtained temperature dependence of the thermal conductivity of  $\text{N}_2\text{O}$  crystal is described by Eq. (1) with expression (7) for  $\tau_r$  at the temperature range below

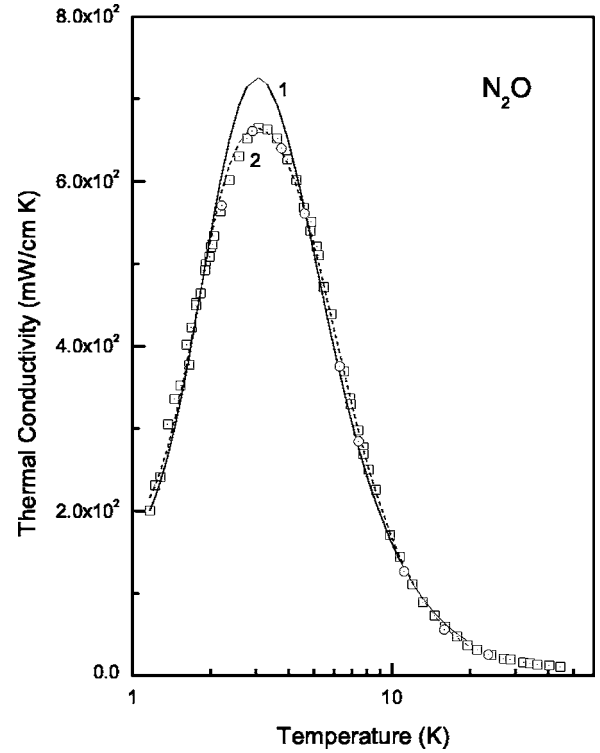


FIG. 4. Low-temperature thermal conductivity of  $\text{N}_2\text{O}$  crystals. Our experimental data:  $\odot$ —the present work,  $\square$ —data from Ref. 13. Fitting curves: 1 (solid)—with  $\tau_r^{-1}$  according to (2), 2 (dotted)—with  $\tau_r^{-1}$  according to (7).

$\sim 20$  K. As a result of the fitting procedure, the relaxation rate of this additional scattering has been found:

$$\tau_a^{-1} = a_a x^\xi T^{2+\xi}, \quad (8)$$

where  $\xi \approx 1/5$ .

Curve 2, depicted in Fig. 4, was obtained as a result of this approximation. As one can see from Fig. 4 curve 2 satisfactorily describes the experimental data in the temperature range below  $\sim 20$  K. The following fitting parameters  $a_j$  have been obtained:

$$\begin{aligned} a_b &= 4.471 \times 10^5 \text{ s}^{-1}, & a_d &= 6.157 \times 10^4 \text{ s}^{-1} \text{ K}^{-1}, \\ a_p &= 5.861 \text{ s}^{-1} \text{ K}^{-4}, & a_{1u} &= 2.884 \times 10^3 \text{ s}^{-1} \text{ K}^{-5}, \\ a_{2u} &= 9.816 \text{ K}, & a_a &= 3.101 \times 10^5 \text{ s}^{-1} \text{ K}^{-11/5}. \end{aligned} \quad (9)$$

The contributions of the relaxation rate ( $\tau_i^{-1}/\tau_r^{-1} = \tau_r/\tau_i$ ) for the different scattering processes  $\tau_i^{-1}$  ( $i=b, d, p, u, a$ ) to the resistive relaxation rate  $\tau_r^{-1}$  for the  $\text{N}_2\text{O}$  crystal versus the phonon energy are depicted in Fig. 5. The index “a” stands for the additional mechanism of scattering of phonons supposedly on end-to-end disordered molecules  $\text{N}_2\text{O}$ . As seen in Fig. 5, the main contribution to the resistive relaxation rate at temperatures below 4 K,  $\tau_r^{-1}$  is provided by the scattering of phonons with energy  $E_{\text{ph}} > \sim 20$  K on point defects and an additional scattering of phonons on disordered molecules  $\text{N}_2\text{O}$ . On the other hand, at higher temperatures, the main contribution to the “resistive” relaxation rate is associated

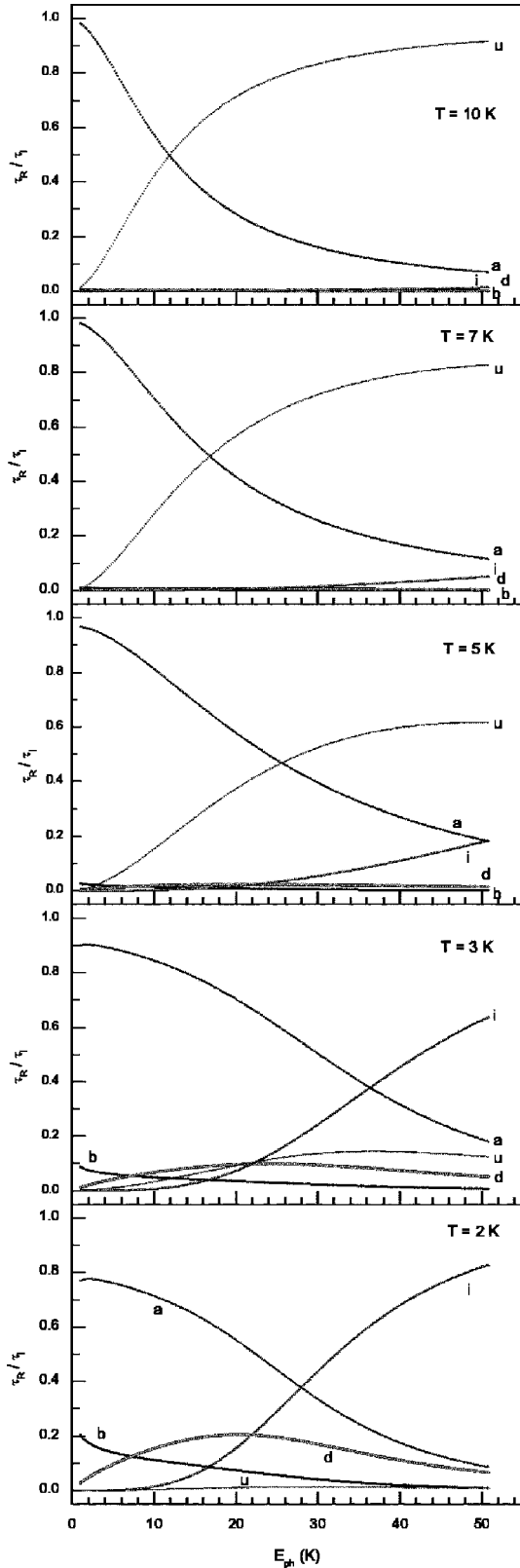


FIG. 5. Ratio of relaxation rate for the individual scattering process  $\tau_i^{-1}$  ( $i=b, d, i, u, a$ ) to the resistive relaxation rate  $\tau_r^{-1}$  at different temperatures for  $N_2O$  crystal versus phonon energy. Scattering of phonons: b—on grain boundaries, d—on dislocation stress fields, i—on point defects, u—on phonons (the U-processes), and a—on molecules of  $N_2O$ , disordered on the O ends.

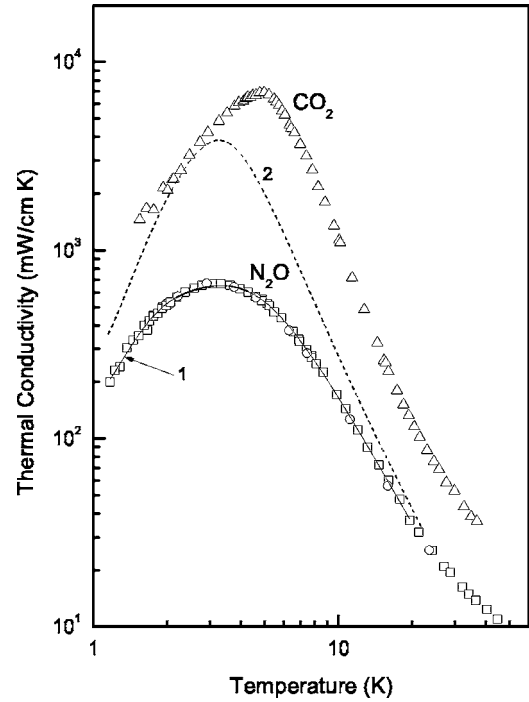


FIG. 6. Low-temperature thermal conductivity of  $CO_2$  and  $N_2O$  crystals. Experiment:  $\triangle$ — $CO_2$ ;  $\square$ — $N_2O$ . The fitting curves: 1 (solid)—with  $\tau_r^{-1}$  according to (7), 2 (dotted)—with  $\tau_r^{-1}$  according to (7) without the last term.

with the scattering of phonons on phonons (U-processes) and the additional scattering.

Using expression (1) for  $\tau_r$  (7) with the last term ( $\tau_a^{-1}$ ) discarded and parameters from (9), one can calculate the dependence of  $\kappa(T)$  for a hypothetical  $N_2O$  crystal with the mechanism of scattering of phonons on the end-to-end disordered molecules turned off. As seen from Fig. 6, curve 2 is close to the experimental curve of  $\kappa(T)$  for  $CO_2$  crystal for temperatures below maximum of thermal conductivity of  $N_2O$  crystal. Therefore, one can conclude that the scattering of phonons on the end-to-end disordered molecules of  $N_2O$  is responsible for the difference in the values of  $\kappa(T)$  for nitrous oxide and carbon dioxide.

As in the case of  $CO_2$ , the average size of crystallites and the densities of dislocations and point defects were estimated using the expressions from Table I. The average dimension of crystallites  $L$  is equal to about 3.8  $\mu m$ , thus being almost equal to the diameter of the sample.

The density of dislocations  $N_d$  has been estimated from Eq. (5) for phonon scattering on strain fields of dislocations.<sup>20</sup> From comparison of the expressions from Table I and (5), using values  $\gamma=2.16$  (Ref. 7) and  $B \sim a$  ( $a=5.6405 \text{ \AA}$ ),<sup>7</sup> the density  $N_d=2 \times 10^8 \text{ cm}^{-2}$  was obtained. Thus obtained value is approximately equal to that of  $CO_2$ .

The point-defect density  $N_p$  was estimated in the same way as for  $CO_2$ . The obtained value,  $N_p \approx 3.5\%$ , is larger than the concentration of isotope impurities. As in the case of  $CO_2$ , overestimating the value of  $N_p$  can be caused by ignoring the vacancy contribution in mass defect, and the contributions associated with the local variations of field constants and local distortions of the lattice in expression (6).

As seen from the analysis of the experimental data for crystal  $\text{CO}_2$  and  $\text{N}_2\text{O}$ , the parameter  $a_{1u}$  amounts to  $1.5\text{--}3 \times 10^3 \text{ s}^{-1} \text{ K}^{-5}$ . The value of this parameter for a simple molecular crystal is of the order of  $10^4 \text{ s}^{-1} \text{ K}^{-5}$  (see, e.g., Refs. 16 and 20). Since the parameter  $a_{1u}$  describes the phonon–phonon interaction in U-processes, the relatively small values obtained might signify relatively weak phonon–phonon interaction in  $\text{CO}_2$  and  $\text{N}_2\text{O}$  crystals. This could explain high thermal conductivity of  $\text{CO}_2$  and  $\text{N}_2\text{O}$  in the high temperature region.

The parameters  $a_d$ , describing the intensity of phonon scattering on dislocations, are relatively close for  $\text{CO}_2$  and  $\text{N}_2\text{O}$  crystals and are more than ten times smaller than those for  $\text{N}_2$  (Ref. 16) (from thermal conductivity studies) and two orders of magnitude greater than those found for argon (from x-ray studies).<sup>23</sup> Thus, the comparative analysis of the experimental data of thermal conductivity of  $\text{CO}_2$  and  $\text{N}_2\text{O}$  crystals indicates that in solid  $\text{N}_2\text{O}$  there is large additional—in comparison with  $\text{CO}_2$ —scattering of phonons at temperatures near the maximum of the thermal conductivity. It has been proposed that additional scattering is caused by the influence of the disorder of molecular ends of  $\text{N}_2\text{O}$  on thermal conductivity in the low temperature range. An expression of dependence of relaxation rate of that phonon scattering on temperature and phonon frequency  $\tau_a^{-1} \sim \omega^{1/5} T^2$  has been found. It describes satisfactorily the experimental results of thermal conductivity of  $\text{N}_2\text{O}$  crystal.

Certainly, the problem of determination of the relaxation rate  $\tau_a^{-1}$  (which describes the influence of disordering of molecular ends of  $\text{N}_2\text{O}$  on thermal conductivity) requires further theoretical investigation. Moreover, in the analysis the  $N$  processes have not been taken into account. Analysis of the influence of the role of  $N$  processes on heat transport in these crystals will be discussed in another paper.

### C. Nitrous oxide and carbon dioxide versus nitrogen

From the above analysis results that the thermal conductivity of crystals of  $\text{CO}_2$  and  $\text{N}_2\text{O}$  would be very close to each other (see Fig. 6) if there was not an additional scattering of phonons in the latter. The additional scattering of phonons we ascribed to the scattering on disordered dipolar nitrous oxide molecules. However, one more question needs to be answered: what is a reason for the significant discrepancy between thermal conductivities of the investigated here three-atom molecule crystals and the crystal of nitrogen? The answer to the question one can get by analyzing the information regarding dissipative processes in separate phonon scat-

tering mechanisms. For nitrogen crystal the parameter  $a_b$  was of order of  $10^7 \text{ s}^{-1}$  (Ref. 16), while the order of the same parameter found here for nitrous oxide and carbon dioxide was  $10^5 \text{ s}^{-1}$ , what means 100 times more effective scattering of phonons in their collisions with grain boundaries in solid  $\text{N}_2$  than in a crystal of  $\text{N}_2\text{O}$  or  $\text{CO}_2$ . Similarly, the parameter  $a_d$  in case of nitrogen crystal is two orders of magnitude greater than that of nitrous oxide and carbon dioxide ( $a_d$  for  $\text{N}_2$  is of order of  $10^6 \text{ s}^{-1} \text{ K}^{-1}$ , see Ref. 16). This means two orders of magnitude stronger scattering of phonons on dislocation strain fields in pure nitrogen crystal than in crystals of nitrous oxide or carbon dioxide. The significant discrepancy of the parameters  $a_b$  and  $a_d$  resulting from different average size of crystallite and density of dislocations in solid  $\text{N}_2$  and  $\text{N}_2\text{O}$  or  $\text{CO}_2$  causes significantly lower thermal conductivity of nitrogen in comparison with nitrous oxide and carbon dioxide at the temperatures below maximum of  $\kappa(T)$ . High-temperature discrepancy of the conductivities results, what was postulated earlier, from weaker phonon-phonon interaction in crystals of  $\text{N}_2\text{O}$  and  $\text{CO}_2$  than that of in  $\text{N}_2$ .

## IV. CONCLUSIONS

Thermal conductivity coefficient of  $\text{CO}_2$  and  $\text{N}_2\text{O}$  crystals has been measured over a temperature range 1–40 K. The developed procedure allowed preparation of high-quality samples of crystalline  $\text{CO}_2$  and  $\text{N}_2\text{O}$ . It was revealed that solid  $\text{CO}_2$  and  $\text{N}_2\text{O}$  exhibit significantly higher thermal conductivity than a typical simple molecular cryocrystal. Relaxation time approximation was applied for an analysis, which took into account phonon scattering on grain boundaries, point defects, dislocation strain fields, and phonons. This approach provides satisfactory description of the data obtained for  $\text{CO}_2$ . The analysis of the experimental data led to the conclusion that in solid  $\text{N}_2\text{O}$  there is an additional, large (in comparison to  $\text{CO}_2$ ) phonon scattering at temperatures near the maximum of the thermal conductivity. The dependence of that scattering of phonons relaxation rate on temperature and phonon frequency was found, which allows satisfactory description of the experimental results of thermal conductivity of  $\text{N}_2\text{O}$  crystal.

## ACKNOWLEDGMENTS

This work was supported by the Polish State Committee for Scientific Research under Contract No. 2P03B 040 25. The authors gratefully thank Yu. A. Freiman for critical reading of the manuscript and fruitful comments.

<sup>1</sup>K. R. Witters and J. E. Cahill, *J. Chem. Phys.* **67**, 2405 (1977).

<sup>2</sup>I. N. Krupskii, A. I. Prokhvatilov, and A. I. Erenburg, *Fiz. Nizk. Temp.* **6**, 1174 (1980) [*Sov. J. Low Temp. Phys.* **6**, 569 (1980)].

<sup>3</sup>T. Atake and H. A. Chihara, *Bull. Chem. Soc. Jpn.* **47**, 2126 (1974).

<sup>4</sup>L. A. Koloskova, I. N. Krupskii, V. G. Manzhelii, B. Ya. Gorodilov, and Yu. G. Kravchenko, *Fiz. Tverd. Tela (Leningrad)* **16**,

3089 (1974) [*Sov. Phys. Solid State* **16**, 1993 (1975)].

<sup>5</sup>Yu. G. Kravchenko and I. N. Krupskii, *Fiz. Nizk. Temp.* **12**, 79 (1986) [*Sov. J. Low Temp. Phys.* **12**, 46 (1986)].

<sup>6</sup>V. A. Konstantinov, V. G. Manzhelii, S. A. Smirnov, and A. N. Tolkachev, *Fiz. Nizk. Temp.* **14**, 189 (1988) [*Sov. J. Low Temp. Phys.* **14**, 104 (1988)].

<sup>7</sup>*Physics of Cryocrystals*, edited by V. G. Manzhelii and Yu. A.

- Freiman (AIP, New York, 1996).
- <sup>8</sup>V. G. Manzhelii, A. I. Prokhvatilov, V. G. Gavrilko, and A. P. Isakina, *Structure and Thermodynamic Properties of Cryocrystals* (Begell House, New York, 1998).
- <sup>9</sup>W. C. Hamilton and M. Petrie, *J. Phys. Chem.* **65**, 1453 (1961).
- <sup>10</sup>M. W. Melhuish and R. L. Scott, *J. Phys. Chem.* **68**, 2301 (1964).
- <sup>11</sup>K. R. Nary, P. L. Kuhns, and M. S. Conradi, *Phys. Rev. B* **26**, 3370 (1982).
- <sup>12</sup>A. M. Tolkachev, V. G. Manzhelii, V. P. Azarenkov, A. Jeżowski, and E. A. Kosobutskaya, *Fiz. Nizk. Temp.* **6**, 1533 (1980) [*Sov. J. Low Temp. Phys.* **6**, 747 (1980)].
- <sup>13</sup>P. Stachowiak, V. V. Sumarokov, J. Mucha, and A. Jeżowski, *Phys. Rev. B* **67**, 172102 (2003).
- <sup>14</sup>V. V. Sumarokov, P. Stachowiak, and A. Jeżowski, *Fiz. Nizk. Temp.* **29**, 603 (2003) [*Low Temp. Phys.* **29**, 449 (2003)].
- <sup>15</sup>A. Jeżowski and P. Stachowiak, *Cryogenics* **32**, 601 (1992).
- <sup>16</sup>P. Stachowiak, V. V. Sumarokov, J. Mucha, and A. Jeżowski, *Phys. Rev. B* **50**, 543 (1994).
- <sup>17</sup>P. Stachowiak, V. V. Sumarokov, J. Mucha, and A. Jeżowski, *J. Low Temp. Phys.* **11**, 379 (1998).
- <sup>18</sup>A. Jeżowski, P. Stachowiak, V. V. Sumarokov, J. Mucha, and Yu. A. Freiman, *Phys. Rev. Lett.* **71**, 97 (1993).
- <sup>19</sup>R. M. Kimber and S. J. Rogers, *J. Phys. C* **6**, 2279 (1973).
- <sup>20</sup>R. Berman, *Thermal Conduction in Solids* (Clarendon, Oxford, 1976).
- <sup>21</sup>T. A. Scott, *Phys. Rep., Phys. Lett.* **27C**, 89 (1976).
- <sup>22</sup>H. B. G. Casimir, *Physica (Utrecht)* **5**, 495 (1938).
- <sup>23</sup>O. G. Peterson, D. N. Batchelder, and R. O. Simmons, *J. Appl. Phys.* **36**, 2682 (1965).